



CPD

10, 105–148, 2014

**Constraining the
*i*LOVECLIM
comparison using
($\delta^{18}\text{O}$)**

T. Caley et al.

Constraining the Last Glacial Maximum climate by data-model (*i*LOVECLIM) comparison using oxygen stable isotopes

T. Caley¹, D. M. Roche^{1,2}, C. Waelbroeck², and E. Michel²

¹Earth and Climate Cluster, Faculty of Earth and Life Sciences, Vrije Universiteit Amsterdam, Amsterdam, the Netherlands

²Laboratoire des Sciences du Climat et de l'Environnement (LSCE), CEA/CNRS-INSU/UVSQ, Gif-sur-Yvette Cedex, France

Received: 29 October 2013 – Accepted: 6 December 2013 – Published: 10 January 2014

Correspondence to: T. Caley (t.caley@vu.nl)

Published by Copernicus Publications on behalf of the European Geosciences Union.

Title Page

Abstract

Introduction

Conclusions

References

Tables

Figures



Back

Close

Full Screen / Esc

Printer-friendly Version

Interactive Discussion



Abstract

We use the fully coupled atmosphere-ocean three-dimensional model of intermediate complexity *i*LOVECLIM to simulate the climate and oxygen stable isotopic signal during the Last Glacial Maximum (LGM, 21 000 yr). By using a model that is able to explicitly simulate the sensor ($\delta^{18}\text{O}$), results can be directly compared with data from climatic archives in the different realms.

Our results indicate that *i*LOVECLIM reproduces well the main feature of the LGM climate in the atmospheric and oceanic components. The annual mean $\delta^{18}\text{O}$ in precipitation shows more depleted values in the northern and southern high latitudes during the LGM. The model reproduces very well the spatial gradient observed in ice core records over the Greenland ice-sheet. We observe a general pattern toward more enriched values for continental calcite $\delta^{18}\text{O}$ in the model at the LGM, in agreement with speleothem data. This can be explained by both a general atmospheric cooling in the tropical and subtropical regions and a reduction in precipitation as confirmed by reconstruction derived from pollens and plant macrofossils.

Data-model comparison for sea surface temperature indicates that *i*LOVECLIM is capable to satisfyingly simulate the change in oceanic surface conditions between the LGM and present. Our data-model comparison for calcite $\delta^{18}\text{O}$ allows investigating the large discrepancies with respect to glacial temperatures recorded by different microfossil proxies in the North Atlantic region. The results argue for a strong mean annual cooling between the LGM and present ($> 6^\circ\text{C}$), supporting the foraminifera transfer function reconstruction but in disagreement with alkenones and dinocyst reconstructions. The data-model comparison also reveals that large positive calcite $\delta^{18}\text{O}$ anomaly in the Southern Ocean may be explained by an important cooling, although the driver of this pattern is unclear. We deduce a large positive $\delta^{18}\text{O}_{\text{sw}}$ anomaly for the north Indian Ocean that contrasts with a large negative $\delta^{18}\text{O}_{\text{sw}}$ anomaly in the China Sea between the LGM and present. This pattern may be linked to changes in the hydrological cycle over these regions.

Constraining the *i*LOVECLIM comparison using ($\delta^{18}\text{O}$)

T. Caley et al.

Title Page

Abstract

Introduction

Conclusions

References

Tables

Figures

⏪

⏩

◀

▶

Back

Close

Full Screen / Esc

Printer-friendly Version

Interactive Discussion



Constraining the iLOVECLIM comparison using ($\delta^{18}\text{O}$)

T. Caley et al.

[Title Page](#)

[Abstract](#)

[Introduction](#)

[Conclusions](#)

[References](#)

[Tables](#)

[Figures](#)

[⏪](#)

[⏩](#)

[◀](#)

[▶](#)

[Back](#)

[Close](#)

[Full Screen / Esc](#)

[Printer-friendly Version](#)

[Interactive Discussion](#)

Our simulation of the deep ocean suggests that changes in $\delta^{18}\text{O}_{\text{sw}}$ between the LGM and present are not spatially homogenous. This is supported by reconstructions derived from pore fluids in deep-sea sediments. The model underestimates the deep ocean cooling thus biasing the comparison with benthic calcite $\delta^{18}\text{O}$ data. Nonetheless, our data-model comparison support a heterogeneous cooling of few degrees (2–4 °C) in the LGM Ocean.

1 Introduction

Oxygen stable isotopes ($\delta^{18}\text{O}$) are among the most widely used/common tools in palaeoclimatology-palaeoceanography. $\delta^{18}\text{O}$ constitutes an important tracer of the hydrological cycle for the different components of the climatic system (ocean, atmosphere, ice sheets) but processes that control the recorded $\delta^{18}\text{O}$ signal are various and complex. Simulation of climate and its associated isotopic signal allow an investigation of these various and complex processes (e.g. Roche et al., 2004a; Lewis et al., 2010).

Water isotopes have been implemented in numerous atmospheric and oceanic general circulation models (Jouzel et al., 1987; Joussame and Jouzel, 1993; Hoffmann et al., 1998; Schmidt, 1998; Paul et al., 1999; Delaygue et al., 2000; Werner et al., 2000, 2011; Noone and Simmonds, 2002; Mathieu et al., 2002; Lee et al., 2007; Yoshimura et al., 2008; Zhou et al., 2008; Tindall et al., 2009; Risi et al., 2010; Xu et al., 2012). However, they have very seldom been used in coupled climate simulations with water isotopes in both the atmospheric and oceanic components, due to computational costs (Schmidt et al., 2007; LeGrande and Schmidt, 2011). We chose here to use an intermediate complexity model to circumvent that limitation, while retaining a full oceanic general circulation model to allow investigating the details of the oceanic response where numerous palaeodata are available.

Water isotopes have been implemented and validated against data for the present day climate in the global three-dimensional model of intermediate complexity

further climatic factors. A promising way of exploiting palaeo-environmental data for climate-model evaluation is to use models that explicitly simulate the sensor. A decisive advantage of isotope-enabled models is their ability to directly simulate measured quantities (in the present case, $\delta^{18}\text{O}$), so that their results can be directly compared with data from the different climatic archives.

In this study, we present a comparison between LGM simulated and measured oxygen isotopes. The results are presented in terms of anomaly between the LGM and the present. The use of anomaly renders absolute values irrelevant; it concerns a purely relative change. We can therefore ignore complications such as species-specific climate variable relationships, vital effect offsets, and calibrations of values measured relative to the VPDB standard to values on the VSMOW scale (Rohling and Cooke, 1999). We consider both the atmospheric and oceanic component and discuss the agreement between data and model results, as well as the processes driving the isotopic signal recorded.

2 Material and method

2.1 LGM boundary conditions

We use the boundary conditions defined in/by the PMIP2 protocol to simulate the LGM climate. Lowered levels of atmospheric greenhouse gas concentrations ($\text{CO}_2 = 185$ ppm, $\text{CH}_4 = 350$ ppb and $\text{NO}_2 = 200$ ppb) are used in agreement with ice-core measurements (Fluckiger et al., 1999; Dällenbach et al., 2000; Monnin et al., 2001). Ice-sheet topography changes are taken from Peltier (2004) and the surface albedo is set accordingly. Orbital parameters correspond to 21 000 yr before present (Berger and Loutre, 1992). To account for the ~ 130 m decrease in sea level relative to present day, the land-sea mask and the oceanic bathymetry are modified (Lambeck and Chappell, 2001). Some variations exist among the PMIP simulations, mainly for the Northern Hemisphere, in the handling of changes in the river basins (Weber et al.,

Constraining the $\delta^{18}\text{O}$ comparison using $\delta^{18}\text{O}$

T. Caley et al.

Title Page

Abstract

Introduction

Conclusions

References

Tables

Figures

⏪

⏩

◀

▶

Back

Close

Full Screen / Esc

Printer-friendly Version

Interactive Discussion



Constraining the *i*LOVECLIM comparison using $\delta^{18}\text{O}$

T. Caley et al.

Title Page

Abstract

Introduction

Conclusions

References

Tables

Figures

⏪

⏩

◀

▶

Back

Close

Full Screen / Esc

Printer-friendly Version

Interactive Discussion

2007), i.e. changes in river routing due to the presence of ice-sheets. In our LGM simulation we included changes in the water routing from the Laurentide ice-sheet over North America and from the Fennoscandian ice sheet over Eurasia. We applied the above forcings to the model's equilibrium state and integrated it until a new equilibrium was reached, after 5000 yr of integration.

Our choice of using the PMIP2 boundary conditions instead of the more recent PMIP3 protocol arise from several considerations: (1) having a state readily comparable to the already published LGM state of an earlier version of the model (Roche et al., 2007), (2) possibility in a future study to intercompare our atmospheric results to already published PMIP2 LGM atmospheric general circulation model, (3) the fact that the main difference between the PMIP2 and PMIP3 protocols is in the ice-sheet elevation (cf. PMIP, 2013) which, interpolated on our atmospheric coarse resolution grid, is not very large.

2.2 Global datasets compilation

Global oxygen isotopic datasets for the atmospheric and oceanic components have been already compiled for the Late Holocene (LH) and have been compared and discussed with *i*LOVECLIM results (Caley and Roche, 2013). Here we compiled $\delta^{18}\text{O}$ data at sites for which the LGM interval is available in order to calculate signal anomalies. Table 1 is a compilation of $\delta^{18}\text{O}$ data from 17 published records from Greenland and Antarctic ice cores. The ice $\delta^{18}\text{O}$ anomalies are reported as the difference between averaged $\delta^{18}\text{O}$ values computed over the period of 20 000–22 000 yr BP and over the last 1000 yr of each record, using published chronologies. For EPICA Dome C and Vostok sites the δD values were converted in $\delta^{18}\text{O}$ values using the global meteoric water line $\delta\text{D} = 8.2 \cdot \delta^{18}\text{O} + 11.27$ (Rozanski et al., 1993). Table 1 also includes calcite $\delta^{18}\text{O}$ data from 10 published speleothem records. Calcite $\delta^{18}\text{O}$ anomalies are reported as the difference between averaged $\delta^{18}\text{O}$ values computed over the period of 20 000–22 000 yr BP and over the last 1000 yr of each record, using published U/Th chronologies.

Constraining the iLOVECLIM comparison using ($\delta^{18}\text{O}$)

T. Caley et al.

Title Page

Abstract

Introduction

Conclusions

References

Tables

Figures

⏪

⏩

◀

▶

Back

Close

Full Screen / Esc

Printer-friendly Version

Interactive Discussion

We compiled calcite $\delta^{18}\text{O}$ measurements from 116 pairs of deep-sea cores for which both LGM and LH planktic foraminifera $\delta^{18}\text{O}$ exist and from 114 pairs of deep-sea cores for which benthic foraminifera $\delta^{18}\text{O}$ exist. Anomalies are reported as the difference between averaged $\delta^{18}\text{O}$ values computed over the period of 19 000–23 000 yr BP and over the last 3000 yr of each record (Tables S1 and S2). Working with anomalies instead of LGM and LH values would reduce uncertainties related to potential changes in planktic foraminifera seasonality or depth habitat (Waelbroeck et al., 2005). We selected marine cores for which the chronology is essentially based on radiogenic dating (^{14}C). Chronostratigraphic quality has been defined following the MARGO project definition (Kucera et al., 2005) (Tables S1 and S2).

Concerning planktic foraminifera, we worked with $\delta^{18}\text{O}$ data of the most commonly measured planktic foraminifer species: *Globigerinoides ruber white* and *pink*, *Globigerinoides sacculifer*, *Globigerina bulloides*, and *Neogloboquadrina pachyderma sinistral* for the majority of the sites. Two exceptions occur at sites MD96-2077 and OCE326-GGC5 for which *Globorotalia inflata* is used (Table S1). We extended our data set with 10 calcite $\delta^{18}\text{O}$ measurements of planktic foraminifera *Neogloboquadrina pachyderma sinistral* compiled by Meland et al. (2005). We only selected records for which the LGM level was determined by AMS ^{14}C and for which LH data (last 3000 yr) was available. These authors used a definition for the LGM chronozone slightly different (18–21.5 ka) but the data allow comparison with model results in the Nordic seas, an area poorly documented in our compilation (Table S1).

Concerning benthic foraminifera $\delta^{18}\text{O}$, we extended our data set with 22 calcite $\delta^{18}\text{O}$ measurements compiled by Zarriess and Mackensen (2011). These authors used a definition for the LGM chronozone (18.3–23.5 ka) that encompasses the one we used (19–23 ka). We also considered four calcite $\delta^{18}\text{O}$ measurements from Adkins et al. (2002) and two calcite $\delta^{18}\text{O}$ measurements from Malone et al. (2004) that have been combined in the same cores with pore fluids measurements in deep-sea sediments to reconstruct deep ocean temperature.

3 Results and discussion

3.1 Atmospheric component

3.1.1 Oxygen stable isotopes in precipitation

In the following we only briefly discuss the annual mean distribution of $\delta^{18}\text{O}$ in precipitation, since a complete description and intercomparison with previously published LGM $\delta^{18}\text{O}$ in precipitation simulations will be undertaken in another study/article in preparation.

Isotopic values are expressed relative to a standard (Sharp, 2007):

$$\delta^{18}\text{O} = R \left(^{18}\text{O} \right)_p / R \left(^{18}\text{O} \right)_{\text{std}} - 1, \quad (1)$$

where R is the abundance ratio of the heavy and light isotopes (e.g., $N(^{18}\text{O})_p/N(^{16}\text{O})_p$) for substance P and δ is commonly reported in units of parts per thousand (‰). The standard for carbonate is Pee Dee Belemnite (PDB) (Craig, 1957) and that for water is Standard Mean Ocean Water (SMOW) (Baertschi, 1976).

Model results for the annual mean precipitation $\delta^{18}\text{O}$ anomaly show large negative values in the northern and southern high latitudes at the LGM compared to the present (Fig. 1). Particularly visible are the area of very depleted $\delta^{18}\text{O}$ precipitation over the imposed LGM ice-sheet in North America and northern Eurasia. In contrast, the mid-latitudes are only slightly depleted and the tropical regions slightly enriched. Over the oceans and with the notable exception of the North Atlantic, the anomaly is relatively symmetric with respect to the equator. Some areas over Siberia exhibit a surprisingly large positive anomaly, despite their increased continentality and the negative $\delta^{18}\text{O}$ anomaly in Western Europe. We do not consider this result as valid but rather, as a result of a model deficiency at very low moisture content, a deficiency that has already been noted for present-day (Roche, 2013).

CPD

10, 105–148, 2014

Constraining the iLOVECLIM comparison using ($\delta^{18}\text{O}$)

T. Caley et al.

Title Page

Abstract

Introduction

Conclusions

References

Tables

Figures

⏪

⏩

◀

▶

Back

Close

Full Screen / Esc

Printer-friendly Version

Interactive Discussion



To compare our model results with isotopic data, we use the precipitation $\delta^{18}\text{O}$ signal from ice cores. We focus on Greenland and Antarctic ice cores (Table 1).

For the Greenland ice-sheet, *i*LOVECLIM model result and data anomalies are in very good agreement ($R^2 = 0.7$) (Fig. 2). A gradient from weak negative $\delta^{18}\text{O}$ anomalies from the North-West (NEEM, Camp Century) through the centre (GRIP, NGRIP) towards large negative $\delta^{18}\text{O}$ anomalies in the South-East (Dye-3) is visible in both data and model results. The maximum depletion occurs in our model over Baffin Bay, with a strong effect of glacial/interglacial sea-ice changes.

Concerning Antarctica, *i*LOVECLIM results are not in good agreement ($R^2 = 0.19$) (Fig. 3, right panel) with the small data set used. Looking in more details at individual ice-core sites, we infer that the model does reproduce qualitatively the east – west gradient in Antarctica, with large negative precipitation $\delta^{18}\text{O}$ anomalies in western Antarctica (Epica Dronning Maud Land, Byrd, WDC, Siple Dome) and smaller negative anomalies in eastern Antarctica. The $\delta^{18}\text{O}$ anomaly at Talos Dome ice core record is well reproduced in the model. Similarly, the values simulated at the Vostok and Dome B sites are not regionally inconsistent. The only ice-core sites that are really at odd with our results are Dome Fuji and Epica Dome C/Dome C data (Table 1 and Fig. 3). Part of the mismatch between the model and the data at those sites may arise from the numerical humidity issue already outlined in Roche (2013).

Some tropical ice cores exist in the Himalayan (Dunde, Guliya) and Andes regions (Huascaran, Sajama and Illimani). The tropics are marked by slightly positive $\delta^{18}\text{O}$ anomalies or no change in *i*LOVECLIM (Fig. 1). The model fails to simulate the depletions ranging from -2 to -5‰ inferred from tropical ice cores (Thompson et al., 1989, 1995, 1998, 2000; Ramirez et al., 2003; Risi et al., 2010). Part of the explanation could reside in the extreme altitude (around 5000–6000 m) of tropical ice cores, hampering a good data-model comparison. Indeed, the altitude in our coarse resolution model for these regions is lower (300 m for the Andes and 4000 m for the Himalayas). Another reason might be the complex precipitation setting of the Andes,

Constraining the *i*LOVECLIM comparison using ($\delta^{18}\text{O}$)

T. Caley et al.

Title Page

Abstract

Introduction

Conclusions

References

Tables

Figures

⏪

⏩

◀

▶

Back

Close

Full Screen / Esc

Printer-friendly Version

Interactive Discussion

with a combination of moisture from the Pacific and recycled moisture from inland regions (Risi et al., 2010).

3.1.2 Oxygen stable isotopes in continental carbonates (speleothems)

Under equilibrium conditions, the $\delta^{18}\text{O}$ of continental carbonates (speleothems) depends on both the temperature through its control on equilibrium fractionation between water and calcite (Hendy, 1971; Kim and O'Neil, 1997) and the isotopic composition of drip water, from the cave site in which the speleothem grew, itself linked to the $\delta^{18}\text{O}$ in precipitation. This relationship between the $\delta^{18}\text{O}$ of carbonates, the $\delta^{18}\text{O}$ of the water, and temperature is expressed by the equation of Kim and O'Neil (1997) for synthetic calcite:

$$\delta^{18}\text{O}_{\text{calcite (speleothem)}} = \delta^{18}\text{O}_{\text{water}} + (18.03 \cdot (1000/T) - 32.17), \quad (2)$$

where T is the temperature in Kelvin.

Although recent works suggest that calcite speleothems do not precipitate under equilibrium conditions (Mickler et al., 2006; Daeron et al., 2011), the use of anomaly calculations between the LGM and LH would limit such potential bias.

As the atmospheric temperature is an important control on the calcite $\delta^{18}\text{O}$ signal, we need to assess the modelled atmospheric temperature. To do so, we used the pollen-based continental climate reconstructions (Bartlein et al., 2011) (Fig. 4). A general cooling during the LGM is observed in both data and model results. Close to the Northern Hemisphere ice sheets the cooling is largest and well reproduced by the model. The LGM cooling indicated by pollen data is more pronounced in southern Europe in comparison to model results. This aspect was already noted (Vandenberghe et al., 2012) and was shown to reflect a too little southward extension of winter sea-ice along the western European coast. It could be attributed to (1) the low resolution of the atmospheric component and (2) the absence of Gibraltar in the oceanic part of the model (Roche and Caley, 2013), promoting warm waters from the Mediterranean along the European coast (Roche et al., 2007; Vandenberghe et al., 2012). In the tropics, the

Constraining the iLOVECLIM comparison using ($\delta^{18}\text{O}$)

T. Caley et al.

Title Page

Abstract

Introduction

Conclusions

References

Tables

Figures

⏪

⏩

◀

▶

Back

Close

Full Screen / Esc

Printer-friendly Version

Interactive Discussion



cooling is reduced compared to the high northern latitudes. With the exception of South Africa where a lot of scatter is observed in the data from a large cooling of -10°C to a moderate -2°C cooling, *i*LOVECLIM reproduces very well the main features of atmospheric temperature between the LGM and present.

5 Simulated atmospheric temperature and precipitation $\delta^{18}\text{O}$ are used to calculate calcite $\delta^{18}\text{O}$. The simulated annual mean anomaly between the LGM and present is then compared to speleothem data (Fig. 5). Considering the error bars on the data (Table 1), we observe overall positive calcite $\delta^{18}\text{O}$ anomalies except for Solufar cave (Fig. 5). As shown previously, mean annual atmospheric temperature are globally
10 cooler during the LGM (Fig. 4). Precipitation reconstruction derived from subfossil pollens and plant macrofossils for the LGM suggests a significant decrease in precipitation compared to present over the Eurasia, Africa and North America (Bartlein et al., 2011). Both the significant cooling and drying of the LGM climate can explain the overall pattern toward positive calcite $\delta^{18}\text{O}$ anomalies. Overall, for nine sites over
15 the ten compiled, there is a very good agreement between data and model results (Fig. 5). In a previous data model comparison study for the late Holocene (Caley and Roche, 2013), we concluded that limitation of the model together with the processes operating in the atmosphere, soil zone, epikarst and cave system hampered a good quantitative data model comparison for the continental calcite $\delta^{18}\text{O}$ signal. The better
20 agreement between data and model results in term of annual mean anomaly suggests that this approach allows us to reduce complications with the atmospheric, soil and cave processes and that the model is capable to reproduce the right amplitude of changes. This offers large perspectives for the understanding of speleothems records covering glacial-interglacial time scale. Indeed, long-term transient simulation of water isotopes with *i*LOVECLIM could be realized and the relationship between the $\delta^{18}\text{O}$
25 precipitation signal and climate variables such as temperature and precipitation rates could be investigated.

Constraining the *i*LOVECLIM comparison using ($\delta^{18}\text{O}$)

T. Caley et al.

[Title Page](#)[Abstract](#)[Introduction](#)[Conclusions](#)[References](#)[Tables](#)[Figures](#)[⏪](#)[⏩](#)[◀](#)[▶](#)[Back](#)[Close](#)[Full Screen / Esc](#)[Printer-friendly Version](#)[Interactive Discussion](#)

3.2 Surface and deep ocean

3.2.1 Oxygen stable isotopes in surface ocean carbonates (planktic foraminifera)

The carbonate isotopic concentration from various organisms such as foraminifera is mainly controlled by temperature and by the isotopic composition of seawater ($\delta^{18}\text{O}_{\text{sw}}$) during shell formation (Urey, 1947; Shackleton, 1974).

The temperature dependence of the equilibrium fractionation of inorganic calcite precipitation around 16.9°C is given in Shackleton (1974) as:

$$T = 16.9 - 4.38(\delta^{18}\text{O}_{\text{carbonate(PDB)}} - \delta^{18}\text{O}_{\text{sw(SMOW)}}) + 0.1(\delta^{18}\text{O}_{\text{carbonate(PDB)}} - \delta^{18}\text{O}_{\text{sw(SMOW)}})^2 \quad (3)$$

As the calcite $\delta^{18}\text{O}$ signal is controlled by temperature and $\delta^{18}\text{O}_{\text{sw}}$, it is important to discuss and assess these variables in our model. The assessment can be carried out for sea surface temperature (SST) using reconstruction of LGM SST derived from different microfossil proxies (MARGO Project Members, 2009). On the contrary, there is currently no method to directly reconstruct surface water $\delta^{18}\text{O}$ in the past.

We observe a very good agreement between simulated and measured SST anomalies between the LGM and the present (Fig. 6). Figure 6b illustrates the data-model agreement or disagreement taking into accounts the uncertainties on LGM SST reconstructions (MARGO Project Members, 2009). Model results confirm that the strongest annual mean cooling occurred in the mid-latitude North Atlantic (MARGO Project Members, 2009). However, some discrepancies between SST reconstructions and model results occur south of Iceland and Greenland. We will discuss in detail this point later in the manuscript. In the tropical band (30°S–30°N) our model results are in excellent agreement with data and therefore confirm that the tropical cooling is more extensive than that proposed by CLIMAP (MARGO Project Members, 2009). Interbasin

CPD

10, 105–148, 2014

Constraining the iLOVECLIM comparison using ($\delta^{18}\text{O}$)

T. Caley et al.

Title Page

Abstract

Introduction

Conclusions

References

Tables

Figures

⏪

⏩

◀

▶

Back

Close

Full Screen / Esc

Printer-friendly Version

Interactive Discussion



differences as well as west-east gradients within each basin, although much weaker in the model, mark the equatorial oceans in agreement with MARGO reconstructions.

After subtraction of the LGM ice-sheets contribution ($\sim 1\%$) (Schrag et al., 1996; Duplessy et al., 2002), modelled surface water $\delta^{18}\text{O}$ anomalies exhibit negative values in the North Atlantic region (between 30 and 60°N) (Fig. 7). This probably reflects the changes in ice-sheets distribution and their impact on surface water $\delta^{18}\text{O}$ through depleted water discharges from rivers. Both sides of the Greenland ice-sheet are marked by positive anomalies (Fig. 7) that reflect the change from present day seasonal sea-ice to LGM permanent sea ice condition in agreement with proxy reconstruction (De vernal et al., 2006). Changes in $\Delta\delta^{18}\text{O}_{\text{sw}}$ are null in the Southern Ocean and the rest of the oceans (tropical area) is mainly marked by slight positive anomalies, probably reflecting the more enriched $\delta^{18}\text{O}$ precipitation signal during the LGM (Fig. 1).

We computed annual mean calcite $\delta^{18}\text{O}$ anomalies from simulated $\delta^{18}\text{O}_{\text{sw}}$ and SST and compared the results with deep-sea core data (Fig. 8). We chose a depth habitat of $0\text{--}50\text{ m}$ to calculate calcite $\delta^{18}\text{O}$ anomalies as we previously demonstrated that it was suitable for a comparison with a global and varied dataset composed of different species of foraminifera (Caley and Roche, 2013). Although ecological effects can also play a role and are more expressed when individual species are considered (Caley and Roche, 2013) our strategy based on anomaly calculation limits such potential biases.

We observe a good qualitative agreement between data and model results (Fig. 8a). Figure 8b illustrates the data-model agreement or disagreement taking into accounts the uncertainties (2σ) on LGM and LH calcite $\delta^{18}\text{O}$ reconstructions (Table S1). Overall, we observe quantitative good agreement between data and model except in the North Indian region. Although calcite $\delta^{18}\text{O}$ anomalies are larger in the model than in the data, the sign of the latitudinal gradient observed in the Indian Ocean is correct (Fig. 8a).

Steep calcite $\delta^{18}\text{O}$ gradients between 30 and 90°N in the Atlantic Ocean are visible (Fig. 8). This is also expressed on a global latitudinal transect as the majority of data northward of 30°N are located in the Atlantic. The calcite $\delta^{18}\text{O}$ anomaly at 30°N is

CPD

10, 105–148, 2014

Constraining the iLOVECLIM comparison using ($\delta^{18}\text{O}$)

T. Caley et al.

Title Page

Abstract

Introduction

Conclusions

References

Tables

Figures

⏪

⏩

◀

▶

Back

Close

Full Screen / Esc

Printer-friendly Version

Interactive Discussion



1‰, then change to 2.5–3‰ between 40 and 60° N and finally decrease between 65 and 90° N (lower than 1‰) (Fig. 9a).

We compare these trends with a global latitudinal transect of Δ SST and the same latitudinal transect for the simulated $\Delta\delta^{18}\text{O}_{\text{sw}}$ (Fig. 9b and c). We conclude that observed calcite $\delta^{18}\text{O}$ gradients in the north Atlantic are mainly an effect of SST changes with latitude. Indeed, large positive calcite $\delta^{18}\text{O}$ anomalies are associated with negative $\delta^{18}\text{O}_{\text{sw}}$ anomalies and colder temperatures indicating the dominant role of SST in driving the calcite $\delta^{18}\text{O}$ signal (Fig. 9).

The data-model comparison also reveals large positive calcite $\delta^{18}\text{O}$ anomalies in the Southern Ocean, between 45 and 50° S (1.5–2‰). In a previous study, we argue that a data-model comparison for calcite $\delta^{18}\text{O}$ in past climate could constitute an interesting way for mapping the potential shifts of the frontal systems and circulation changes through time, in particular in the Southern region (Caley and Roche, 2013). The large values observed are linked to a large negative SST anomaly in the region with weak changes in $\Delta\delta^{18}\text{O}_{\text{sw}}$ observed in our model (Fig. 9). The cooling could be directly linked to the reorganisation of frontal systems during glacial periods as documented in many studies (Peeters et al., 2004; Bard and Rickaby, 2009; Caley et al., 2012). However the driver of this potential fronts reorganisation is far from being understood. It could be related to SH westerlies changes, although recent data-model comparison works have no clear conclusion on the behaviour of westerlies during the LGM (Kohfeld et al., 2013; Sime et al., 2013). It is interesting to note that the Southern Ocean, subtropical South Atlantic and Pacific are regions where large disagreements occur among the latest coupled-GCM LGM simulations (Braconnot et al., 2007a). The fact that *i*LOVECLIM reproduces well the observed cooling and the main pattern of the calcite $\delta^{18}\text{O}$ signal in the Southern region illustrates how data-model comparison for oxygen isotopes can serve to evaluate model's capability to simulate a climate that is drastically different from that of the present-day.

The tropical regions (30° N–30° S) exhibit overall a large positive calcite $\delta^{18}\text{O}$ anomaly of 1–2‰ that mainly reflects a negative SST anomaly (Figs. 9 and 10). An

CPD

10, 105–148, 2014

Constraining the *i*LOVECLIM comparison using ($\delta^{18}\text{O}$)

T. Caley et al.

Title Page

Abstract

Introduction

Conclusions

References

Tables

Figures

⏪

⏩

◀

▶

Back

Close

Full Screen / Esc

Printer-friendly Version

Interactive Discussion



Constraining the iLOVECLIM comparison using ($\delta^{18}\text{O}$)

T. Caley et al.

Title Page

Abstract

Introduction

Conclusions

References

Tables

Figures

⏪

⏩

◀

▶

Back

Close

Full Screen / Esc

Printer-friendly Version

Interactive Discussion

exception occurs in the North Indian Ocean for which we observed a higher calcite $\delta^{18}\text{O}$ anomaly (2–3‰). This anomaly can not be explained by the cooling observed in the region but rather by a higher $\Delta\delta^{18}\text{Osw}$ (Figs. 9 and 10). Indeed, the cooling in the tropical Atlantic is more pronounced than in the north Indian Ocean but the calcite $\delta^{18}\text{O}$ anomaly is not larger (Fig. 10). This large positive anomaly observed in data for the North Indian Ocean is overestimated in the model (Figs. 8, 9 and 10). This is probably due to the anomalously low $\delta^{18}\text{Osw}$ signal simulated by the model for the present day in the North Indian region (Roche and Caley, 2013). Explanations for the observed North Indian Ocean enrichment in $\delta^{18}\text{Osw}$ at the LGM could be (1) a contraction of the Indian subtropical gyre and reduction of Agulhas leakage salty water (Caley et al., 2011a) and/or (2) an overall reduction of the hydrological cycle over the western and northern Asian region, in agreement with numerous Indo-Asian monsoonal reconstructions (Schultz et al., 1998; Iwamoto and Inouchi, 2007; Cheng et al., 2009; Guo et al., 2009; Caley et al., 2011b, c; Chabangborn et al., 2013).

Also interesting is the low calcite $\delta^{18}\text{O}$ anomaly observed in the China Sea (Figs. 8 and 10). This signal cannot be explained by a temperature effect as we observe a cooling more important in the China Sea in comparison to the North Indian Ocean (Figs. 6 and 10). Therefore, we hypothesize an important decrease of the $\Delta\delta^{18}\text{Osw}$, a pattern exhibited in our model (Fig. 10c). The cause for such important decrease of the $\Delta\delta^{18}\text{Osw}$ is not completely clear because the monsoon in East Asia is rather reduced during the LGM (Iwamoto and Inouchi, 2007; Cheng et al., 2009; Guo et al., 2009). Nonetheless, some studies argue for substantial precipitation during the LGM in South China sea (Sun et al., 2000; Colin et al., 2010; Chabangborn et al., 2013). Indeed, part of the explanation could reside in the negative $\delta^{18}\text{O}$ anomaly observed in precipitation over the China Sea (Fig. 1).

The use of calcite $\delta^{18}\text{O}$ anomalies in the tropical regions (30° N–30° S) do not allow the confirmation of the presence of west-east SST gradients within each basin as the amount of data is rather limited.

disagreement with reconstructions based on $\delta^{13}\text{C}$ and Cd/Ca proxies (Lynch-Stieglitz et al., 2007 and references therein) and with our model results.

Qualitative and quantitative comparison of calcite $\delta^{18}\text{O}$ anomaly, calculated with the model and benthic foraminifera data with associated error bars (2σ) (Table S2), are visible on Fig. 13a–d for the deep Atlantic and Pacific Oceans. Some discrepancies can be observed between data and model and are particularly marked in the equatorial Atlantic at ~ 1000 m, the deep Southern Ocean and central Pacific. The calcite $\delta^{18}\text{O}$ anomaly is influenced by temperature. The modelled deep-water temperature for the present is around 2°C lower than data, a pattern particularly marked in the Southern Ocean (Caley and Roche, 2013). This introduces bias in our data-model comparison. The uses of anomalies only slightly limit such bias because deep LGM temperatures are close to the freezing point of seawater at the ocean's surface (Adkins et al., 2002).

Reconstructions of past deep temperature are rather rare and localised. The north Atlantic, South Indian and equatorial Pacific are marked by negative temperature anomalies of ~ 4 , 3 and 2°C respectively between the LGM and present (Adkins et al., 2002; Waelbroeck et al., 2002; Siddall et al., 2010) (Fig. 13e and f). Similarly, reconstruction of deep temperature anomaly in the South Pacific yields $\sim 2^\circ\text{C}$ (Malone et al., 2004; Elderfield et al., 2012) (Fig. 13f). The modelled deep temperature anomalies are in good agreement for the North Atlantic at 2000 but not at 4500 m as for the $\delta^{18}\text{O}_{\text{sw}}$ anomaly. For the Southern Ocean and deep equatorial Pacific, the negative anomalies between the LGM and present are about 1°C too weak in the model (Fig. 13f).

Although there are some discrepancies between modelled and measured deep-water temperature, our data model comparison support a heterogeneous cooling of few degrees ($2\text{--}4^\circ\text{C}$) in the LGM Ocean.

CPD

10, 105–148, 2014

Constraining the iLOVECLIM comparison using ($\delta^{18}\text{O}$)

T. Caley et al.

Title Page

Abstract

Introduction

Conclusions

References

Tables

Figures

⏪

⏩

◀

▶

Back

Close

Full Screen / Esc

Printer-friendly Version

Interactive Discussion

4 Conclusions

We used the fully coupled atmosphere-ocean three-dimensional model of intermediate complexity *i*LOVECLIM to simulate the climate and oxygen stable isotopes ($\delta^{18}\text{O}$) in the atmospheric and oceanic component during the LGM. We also realized a careful compilation of global oxygen isotopic datasets to assess the model performance and constrain the LGM climate. Model results for the annual mean precipitation $\delta^{18}\text{O}$ show more depleted values in the northern and southern high latitudes during the LGM than at present. The simulated spatial gradient in precipitation $\delta^{18}\text{O}$ over Greenland is in very good agreement with ice core records, whereas simulated values are in less good agreement with data over Antarctica. We observe a general pattern toward more enriched calcite $\delta^{18}\text{O}$ in the model over the continents at the LGM, in agreement with speleothem data. This can be explained by both a general atmospheric cooling in the tropical and subtropical regions and a reduction in precipitation, as confirmed by reconstructions derived from pollens and plant macrofossils (Bartlein et al., 2011). The good agreement between data and model results in term of annual mean calcite $\delta^{18}\text{O}$ anomaly offers large perspectives for the understanding of speleothems records covering glacial-interglacial time scale. Long-term transient simulations of water isotopes with *i*LOVECLIM are planned in the near future and the relationship between precipitation $\delta^{18}\text{O}$ and climate variables such as temperature and precipitation will be investigated.

Data-model comparison for sea surface temperature indicates that *i*LOVECLIM is capable to satisfyingly simulate oceanic surface conditions at the LGM, whereas the majority of AO-GCM simulations experience some difficulties (Braconnot et al., 2007a). Large discrepancies with respect to glacial temperatures recorded by different microfossil proxies remain in the North Atlantic region and there was no objective way to reconcile the divergent proxy results (MARGO Project Members, 2009). Our data-model comparison for planktic foraminiferal calcite $\delta^{18}\text{O}$ indicates that a strong mean annual cooling characterized the LGM with respect to the present ($> 6^\circ\text{C}$), supporting

CPD

10, 105–148, 2014

Constraining the *i*LOVECLIM comparison using ($\delta^{18}\text{O}$)

T. Caley et al.

Title Page

Abstract

Introduction

Conclusions

References

Tables

Figures

⏪

⏩

◀

▶

Back

Close

Full Screen / Esc

Printer-friendly Version

Interactive Discussion

Constraining the *i*LOVECLIM comparison using ($\delta^{18}\text{O}$)

T. Caley et al.

Title Page

Abstract

Introduction

Conclusions

References

Tables

Figures

⏪

⏩

◀

▶

Back

Close

Full Screen / Esc

Printer-friendly Version

Interactive Discussion

the foraminifera transfer function reconstruction but in disagreement with alkenones and dinocyst reconstructions. The data-model comparison also reveals large positive calcite $\delta^{18}\text{O}$ anomalies in the Southern Ocean linked to an important cooling that could be linked to a reorganization of frontal systems during the LGM. Nonetheless, the exact driver of this pattern remains unclear. From our data-model comparison of planktic foraminifer oxygen stable isotopes and SST we deduced a large positive/negative $\delta^{18}\text{O}_{\text{sw}}$ anomaly for the north Indian Ocean/China Sea between the LGM and present which may be explained by changes in the hydrological cycle over the region.

Our simulation of the deep ocean suggests that changes in $\delta^{18}\text{O}_{\text{sw}}$ between the LGM and present are not spatially homogenous. This is supported by reconstructions derived from pore fluids in deep-sea sediments. The model underestimates the deep ocean cooling thus biasing the comparison with benthic calcite $\delta^{18}\text{O}$ data. Some experiments are planned in a near future to try modifying this aspect in the model. Nonetheless, our data model comparison support a heterogeneous cooling of few degrees (2–4 °C) in the LGM Ocean.

*i*LOVECLIM reproduces well the $\delta^{18}\text{O}$ signals between the LGM and present and therefore illustrates how data-model comparison for oxygen isotopes can serve to evaluate model's capability to simulate a climate that is drastically different from that of the present-day.

Supplementary material related to this article is available online at <http://www.clim-past-discuss.net/10/105/2014/cpd-10-105-2014-supplement.pdf>.

Acknowledgements. T. Caley is supported by NWO through the VIDI/AC²ME project no 864.09.013. D. M. Roche is supported by NWO through the VIDI/AC²ME project no. 864.09.013 and by CNRS-INSU. Institut Pierre Simon Laplace is gratefully acknowledged for hosting the *i*LOVECLIM model code under the LUDUS framework project (<https://forge.ipsl.jussieu.fr/ludus>). This is NWO/AC²ME contribution number 04.

References

- Adkins, J. F., McIntyre, K., and Schrag, D.: The salinity, temperature and $\delta^{18}\text{O}$ of the glacial deep ocean, *Science*, 298, 1769–1773, 2002.
- Baertschi, P.: Absolute ^{18}O content of Standard Mean Ocean Water, *Earth Planet. Sc. Lett.*, 31, 341–44, 1976.
- Bard, E. and Rickaby, E. M.: Migration of the subtropical front as a modulator of glacial climate, *Nature*, 460, 380–383, 2009.
- Bartlein, P. J., Harrison, S. P., Brewer, S., Connor, S., Davis, B. A. S., Gajewski, K., Guiot, J., Harrison-Prentice, T. I., Henderson, A., Peyron, O., Prentice, I. C., Scholze, M., Seppa, H., Shuman, B., Sugita, S., Thompson, R. S., Viau, A. E., Williams, J., and Wu, H.: Pollen-based continental climate reconstructions at 6 and 21 ka: a global synthesis, *Clim. Dynam.*, 37, 775–802, doi:10.1007/s00382-010-0904-1, 2011.
- Benthien, A. and Müller, P. J.: Anomalously low alkenone temperatures caused by lateral particle and sediment transport in the Malvinas Current region, western Argentine Basin, *Deep-Sea Res. Pt. I*, 47, 2369–2393, 2000.
- Berger, A. and Loutre, M.: Astronomical solutions for palaeoclimate studies over the last 3 millions years, *Earth Planet. Sc. Lett.*, 111, 369–382, 1992.
- Boyle, E. A.: Cool tropical temperatures shift the global $\delta^{18}\text{O}$ -T relationship: an explanation for the ice core $\delta^{18}\text{O}$ -borehole thermometry conflict?, *Geophys. Res. Lett.*, 24, 273–276, 1997.
- Braconnot, P., Otto-Bliesner, B., Harrison, S., Joussaume, S., Peterchmitt, J.-Y., Abe-Ouchi, A., Crucifix, M., Driesschaert, E., Fichefet, Th., Hewitt, C. D., Kageyama, M., Kitoh, A., Laîné, A., Loutre, M.-F., Marti, O., Merkel, U., Ramstein, G., Valdes, P., Weber, S. L., Yu, Y., and Zhao, Y.: Results of PMIP2 coupled simulations of the Mid-Holocene and Last Glacial Maximum – Part 1: experiments and large-scale features, *Clim. Past*, 3, 261–277, doi:10.5194/cp-3-261-2007, 2007a.
- Braconnot, P., Otto-Bliesner, B., Harrison, S., Joussaume, S., Peterchmitt, J.-Y., Abe-Ouchi, A., Crucifix, M., Driesschaert, E., Fichefet, Th., Hewitt, C. D., Kageyama, M., Kitoh, A., Loutre, M.-F., Marti, O., Merkel, U., Ramstein, G., Valdes, P., Weber, L., Yu, Y., and Zhao, Y.: Results of PMIP2 coupled simulations of the Mid-Holocene and Last Glacial Maximum – Part 2: Feedbacks with emphasis on the location of the ITCZ and mid- and high latitudes heat budget, *Clim. Past*, 3, 279–296, doi:10.5194/cp-3-279-2007, 2007b.

CPD

10, 105–148, 2014

Constraining the iLOVECLIM comparison using ($\delta^{18}\text{O}$)

T. Caley et al.

[Title Page](#)

[Abstract](#)

[Introduction](#)

[Conclusions](#)

[References](#)

[Tables](#)

[Figures](#)

[⏪](#)

[⏩](#)

[◀](#)

[▶](#)

[Back](#)

[Close](#)

[Full Screen / Esc](#)

[Printer-friendly Version](#)

[Interactive Discussion](#)

Constraining the i/LOVECLIM comparison using ($\delta^{18}\text{O}$)

T. Caley et al.

[Title Page](#)

[Abstract](#)

[Introduction](#)

[Conclusions](#)

[References](#)

[Tables](#)

[Figures](#)

[⏪](#)

[⏩](#)

[◀](#)

[▶](#)

[Back](#)

[Close](#)

[Full Screen / Esc](#)

[Printer-friendly Version](#)

[Interactive Discussion](#)

Braconnot, P., Harrison, S. P., Kageyama, M., Bartlein, P. J., Masson-Delmotte, V., Abe-Ouchi, A., Otto-Bliesner, B., and Zhao, Y.: Evaluation of climate models using palaeoclimatic data, *Nature Climate Change*, 2, 417–424, doi:10.1038/nclimate1456, 2012.

Caley, T. and Roche, D. M.: $\delta^{18}\text{O}$ water isotope in the i/LOVECLIM model (version 1.0) – Part 3: A palaeo-perspective based on present-day data–model comparison for oxygen stable isotopes in carbonates, *Geosci. Model Dev.*, 6, 1505–1516, doi:10.5194/gmd-6-1505-2013, 2013.

Caley, T., Kim, J.-H., Malaizé, B., Giraudeau, J., Laepple, T., Caillon, N., Charlier, K., Rebaubier, H., Rossignol, L., Castañeda, I. S., Schouten, S., and Sinninghe Damsté, J. S.: High-latitude obliquity as a dominant forcing in the Agulhas current system, *Clim. Past*, 7, 1285–1296, doi:10.5194/cp-7-1285-2011, 2011a.

Caley, T., Malaize, B., Zaragosi, S., Rossignol, L., Bourget, J., Eynaud, F., Martinez, P., Giraudeau, J., Charlier, K., and Ellouz-Zimmermann, N.: New Arabian Sea records help decipher orbital timing of Indo-Asian monsoon, *Earth Planet. Sc. Lett.*, 308, 433–444, doi:10.1016/j.epsl.2011.06.019, 2011b.

Caley, T., Malaizé, B., Revel, M., Ducassou, E., Wainer, K., Ibrahim, M., Shoeaib, D., Migeaon, S., and Marieu, V.: Orbital timing of the Indian, East Asian and African boreal monsoons and the concept of a “global monsoon”. *Quaternary Sci. Rev.*, 30, 3705–3715, 2011c.

Caley, T., Giraudeau, J., Malaizé, B., Rossignol, L., and Pierre, C.: Agulhas leakage as a key process in the modes of Quaternary climate changes, *P. Natl. Acad. Sci. USA*, 109, 6835–6839, 2012.

Chabangborn, A., Brandefelt, J., and Wohlfarth, B.: Asian monsoon climate during the Last Glacial Maximum: palaeo-data–model comparisons, *Boreas*, 43, 220–242, doi:10.1111/bor.12032, 2013.

Cheng, H., Edwards, R. L., Broecker, W. S., Denton, G. H., Kong, X., Wang, Y., Zhang, R., and Wang, X.: Ice age terminations, *Science*, 326, 248–252, 2009.

CLIMAP: Seasonal reconstructions of the Earth’s surface at the last glacial maximum, *Map and Chart Ser. #36 ed.*, Geological Society of America, 1981.

Colin, C., Siani, G., Sicre, M. A., and Liu, Z.: Impact of the East Asian monsoon rainfall changes on the erosion of the Mekong River basin over the past 25,000 yr, *Mar. Geol.*, 271, 84–92, 2010.

**Constraining the
iLOVECLIM
comparison using
($\delta^{18}\text{O}$)**

T. Caley et al.

[Title Page](#)[Abstract](#)[Introduction](#)[Conclusions](#)[References](#)[Tables](#)[Figures](#)[⏪](#)[⏩](#)[◀](#)[▶](#)[Back](#)[Close](#)[Full Screen / Esc](#)[Printer-friendly Version](#)[Interactive Discussion](#)

- Conte, M. H., Thompson, A., Lesley, D., and Harris, R. P.: Genetic and physiological influences on the alkenone/alkenoate versus growth temperature relationship in *Emiliana huxleyi* and *Gephyrocapsa oceanica*, *Geochim. Cosmochim. Ac.*, 62, 51–68, 1998.
- Conte, M. H., Weber, J. C., King, L. L., and Wakeham, S. G.: The alkenone temperature signal in western North Atlantic surface waters, *Geochim. Cosmochim. Ac.*, 65, 4275–4287, 2001.
- Conte, M. H., Sicre, M. A., Rühlemann, C., Weber, J. C., Schulte, S., Schulz-Bull, D., and Blanz, T.: Global temperature calibration of the alkenone unsaturation index (UK'37) in surface waters and comparison with surface sediments, *Geochem. Geophys. Geosy.*, 7, Q02005, doi:10.1029/2005GC001054, 2006.
- Craig, H.: Isotopic standards for carbon and oxygen and correction factors for mass-spectrometric analysis of carbon dioxide, *Geochim. Cosmochim. Ac.*, 12, 133–149, 1957.
- Crucifix, M., Braconnot, P., Harrison, S., and Otto-Bliesner, B.: Second phase of palaeoclimate modelling intercomparison project, *EOS T. Am. Geophys. Un.*, 86, 264–265, 2005.
- Däeron, M., Guo, W., Eiler, J., Genty, D., Blamart, D., Boch, R., Drysdale, R., Maire, K., Wainer, G., and Zanchetta, G.: $^{13}\text{C}^{18}\text{O}$ clumping in speleothems: observations from natural caves and precipitation experiments, *Geochim. Cosmochim. Ac.*, 75, 3303–3317, 2011.
- Dällenbach, A., Blunier, T., Fluckiger, J., Stauffer, B., Chappellaz, J., and Raynaud, D.: Changes in the atmospheric CH_4 gradient between Greenland and Antarctica during the Last Glacial and the transition to the Holocene, *Geophys. Res. Lett.*, 27, 1005–1008, doi:10.1029/1999GL010873, 2000.
- Delaygue, G., Jouzel, J., and Dutay, J. C.: Oxygen 18-salinity relationship simulated by an oceanic general circulation model, *Earth Planet. Sc. Lett.*, 178, 113–123, doi:10.1016/S0012-821X(00)00073-X, 2000.
- De Vernal, A., Rosell-Melé, A., Kucera, M., Hillaire-Marcel, C., Eynaud, F., Weinelt, M., Dokken, T., and Kageyama, M.: Comparing proxies for the reconstruction of LGM sea-surface conditions in the northern North Atlantic, *Quaternary Sci. Rev.*, 25, 2820–2834, 2006.
- Duplessy, J. C., Labeyrie, L., and Waelbroeck, C.: Constraints on the ocean oxygen isotopic enrichment between the Last Glacial Maximum and the Holocene: paleoceanographic implications, *Quaternary Sci. Rev.*, 21, 315–330, 2002.
- Elderfield, H., Ferretti, P., Greaves, M., Crowhurst, S., McCave, I. N., Hodell, D., and Piotrowski, A. M.: Evolution of ocean temperature and ice volume through the Mid-Pleistocene climate transition, *Science*, 337, 704–709, 2012.

Constraining the iLOVECLIM comparison using ($\delta^{18}\text{O}$)

T. Caley et al.

Title Page

Abstract

Introduction

Conclusions

References

Tables

Figures

⏪

⏩

◀

▶

Back

Close

Full Screen / Esc

Printer-friendly Version

Interactive Discussion

- Fluckiger, J., Dällenbach, A., Blunier, T., Stauffer, B., Stocker, T., Raynaud, D., and Barnola, J.-M.: Variations in atmospheric N_2O concentration during abrupt climatic changes, *Science*, 285, 227–230, doi:10.1126/science.285.5425.227, 1999.
- Guo, Z. T., Berger, A., Yin, Q. Z., and Qin, L.: Strong asymmetry of hemispheric climates during MIS-13 inferred from correlating China loess and Antarctica ice records, *Clim. Past*, 5, 21–31, doi:10.5194/cp-5-21-2009, 2009.
- Hendy, C. H.: The isotopic geochemistry of speleothems, 1. The calculation of the effects of different modes of formation on the isotopic composition of speleothems and their applicability as palaeoclimatic indicators, *Geochim. Cosmochim. Ac.*, 35, 801–824, 1971.
- Hoffmann, G., Werner, M., and Heimann, M.: Water isotope module of the ECHAM atmospheric general circulation model: a study on timescales from days to several years, *J. Geophys. Res.*, 103, 16871–16896, 1998.
- Iwamoto, N. and Inouchi, Y.: Reconstruction of millennial-scale variations in the East Asian summer monsoon over the past 300 ka based on the total carbon content of sediment from Lake Biwa, Japan, *Environ. Geol.*, 52, 1607–1616, 2007.
- Joussaume, S. and Jouzel, J.: Palaeoclimatic tracers: an investigation using an atmospheric general circulation model under ice age conditions: 2. Water isotopes, *J. Geophys. Res.*, 98, 2807–2830, 1993.
- Joussaume, S. and Taylor, K.: Palaeoclimate Modelling Intercomparison Project (PMIP), WCRP-111, WMO/TD-No. 1007, 9–24, 2000.
- Jouzel, J., Koster, R. D., Suozzo, R. J., Russel, G. L., White, J. W. C., and Broecker, W. S.: Simulations of the HDO and H_2^{18}O atmospheric cycles using the NASA GISS General Circulation Model: the seasonal cycle for present-day conditions, *J. Geophys. Res.*, 92, 14739–14760, 1987.
- Kim, S.-T. and O’Neil, J. R.: Equilibrium and nonequilibrium oxygen isotope effects in synthetic carbonates, *Geochim. Cosmochim. Ac.*, 61, 3461–3475, 1997.
- Kohfeld, K. E., Graham, R. M., de Boer, A. M., Sime, L. C., Wolff, E. W., Le Quéré, C., and Bopp, L.: Southern Hemisphere westerly wind changes during the Last Glacial Maximum: paleo-data synthesis, *Quaternary Sci. Rev.*, 68, 76–95, 2013.
- Kucera, M., Rosell-Melé, A., Schneider, R., Waelbroeck, C., and Weinelte, M.: Multiproxy approach for the reconstruction of the glacial ocean surface (MARGO), *Quaternary Sci. Rev.*, 24, 813–819, doi:10.1016/j.quascirev.2004.07.017, 2005.

Constraining the iLOVECLIM comparison using ($\delta^{18}\text{O}$)

T. Caley et al.

Title Page

Abstract

Introduction

Conclusions

References

Tables

Figures

⏪

⏩

◀

▶

Back

Close

Full Screen / Esc

Printer-friendly Version

Interactive Discussion

- Lambeck, K. and Chappell, J.: Sea level change through the Last Glacial Cycle, *Science*, 292, 679–686, 2001.
- Lee, J.-E., Fung, I., DePaolo, D., and Fennig, C. C.: Analysis of the global distribution of water isotopes using the NCAR atmospheric general circulation model, *J. Geophys. Res.*, 112, D16306, doi:10.1029/2006JD007657, 2007.
- LeGrande, A. N. and Schmidt, G. A.: Water isotopologues as a quantitative palaeosalinity proxy, *Palaeoceanography*, 26, PA3225, doi:10.1029/2010PA002043, 2011.
- Lewis, S. C., LeGrande, A. N., Kelley, M., and Schmidt, G. A.: Water vapour source impacts on oxygen isotope variability in tropical precipitation during Heinrich events, *Clim. Past*, 6, 325–343, doi:10.5194/cp-6-325-2010, 2010.
- Lynch-Stieglitz, J., Adkins, J. F., Curry, W. B., Dokken, T., Hall, I. R., Herguera, J. C., Hirschi, J. J. M., Ivanova, E. V., Kissel, C., Marchal, O., Marchitto, T. M., McCave, I. N., McManus, J. F., Mulitza, S., Ninnemann, U., Peeters, F., Yu, E.-F., and Zahn, R.: Atlantic meridional overturning circulation during the Last Glacial Maximum, *Science*, 316, 66–69, 2007.
- Malone, M. J., Martin, J. B., Schönfeld, J., Ninnemann, U. S., Nürnberg, D., and White, T. S.: The oxygen isotopic composition and temperature of Southern Ocean bottom waters during the last glacial maximum, *Earth Planet. Sc. Lett.*, 222, 275–283, 2004.
- MARGO Project Members, Waelbroeck, C., Paul, A., Kucera, M., Rosell-Melee, A., Weinelt, M., Schneider, R., Mix, A. C., Abelman, A., Armand, L., Bard, E., Barker, S., Barrows, T. T., Benway, H., Cacho, I., Chen, M. T., Cortijo, E., Crosta, X., de Vernal, A., Dokken, T., Duprat, J., Elderfield, H., Eynaud, F., Gersonde, R., Hayes, A., Henry, M., Hillaire-Marcel, C., Huang, C. C., Jansen, E., Juggins, S., Kallel, N., Kiefer, T., Kienast, M., Labeyrie, L., Leclaire, H., Londeix, L., Mangin, S., Matthiessen, J., Marret, F., Meland, M., Morey, A. E., Mulitza, S., Pflaumann, U., Pisias, N. G., Radi, T., Rochon, A., Rohling, E. J., Saffi, L., Schafer-Neth, C., Solignac, S., Spero, H., Tachikawa, K., Turon, J. L., and Members, M. P.: Constraints on the magnitude and patterns of ocean cooling at the Last Glacial Maximum, *Nat. Geosci.*, 2, 127–132, 2009.
- Mathieu, R., Pollard, D., Cole, J., White, J. W. C., Webb, R. S., and Thompson, S. L.: Simulation of stable water isotope variations by the GENESIS GCM for modern conditions, *J. Geophys. Res.*, 107, 4037, doi:10.1029/2001JD900255, 2002.
- Meland, M. Y., Jansen, E., and Elderfield, H.: Constraints on SST estimates for the Northern North Atlantic/Nordic Seas during the LGM, *Quaternary Sci. Rev.*, 24, 835–852, 2005.

Constraining the i/LOVECLIM comparison using ($\delta^{18}\text{O}$)

T. Caley et al.

Title Page

Abstract

Introduction

Conclusions

References

Tables

Figures

⏪

⏩

◀

▶

Back

Close

Full Screen / Esc

Printer-friendly Version

Interactive Discussion



- Mickler, P., Stern, L., and Banner, J.: Large kinetic isotope effects in modern speleothems, *Geol. Soc. Am. Bull.*, 118, 65–81, 2006.
- Mix, A. C., Bard, E., and Schneider, R.: Environmental Processes of the Ice Age: Land, Oceans, Glaciers (EPILOG), *Quaternary Sci. Rev.*, 20, 627–657, 2001.
- 5 Mollenhauer, G., McManus, J. F., Benthien, A., Müller P. J. and Eglinton, T. I.: Rapid lateral particle transport in the Argentine Basin: molecular ^{14}C and $^{230}\text{Th}_{\text{xs}}$ evidence, *Deep-Sea Res. Pt. I*, 53, 1224–1243, 2006.
- Monnin, E., Indermuele, A., Daellenbach, A., Flueckiger, J., Stauffer, B., Stocker, T., Raynaud, D., and Barnola, J.-M.: Atmospheric CO_2 concentrations over the Last Glacial
- 10 termination, *Science*, 291, 112–114, 2001.
- Noone, D. and Simmonds, I.: Associations between $\delta^{18}\text{O}$ of water and climate parameters in a simulation of atmospheric circulation for 1979–95, *J. Climate*, 15, 3150–3169, 2002.
- Paul, A., Mulitza, S., Patzold, J., and Wolff, T.: Simulation of oxygen isotopes in a global ocean model, in: *Use of Proxies in Palaeoceanography: examples from the South Atlantic*, edited by: Fischer, G. and Wefer, G., Springer, New York, 655–686, 1999.
- 15 Peltier, W.: Global Glacial Isostasy and the Surface of the Ice-Age Earth: the ICE-5G (VM2) Model and GRACE, *Annu. Rev. Earth Pl. Sc.*, 32, 111–149, doi:10.1146/annurev.earth.32.082503.144359, 2004.
- Peeters, F., Acheson, R., Brummer, G. J. A., de Ruijter, W. P. M., Schneider, R. R., Ganssen, G. M., Ufkes, E., and Kroon, D.: Vigorous exchange between the Indian and Atlantic oceans at the end of the past five glacial periods, *Nature*, 430, 661–665, 2004.
- PMIP (The Paleoclimate Modelling Intercomparison Project): available at: <http://pmip3.lscce.ipsl.fr>, last access: January 2014, 2013.
- Ramirez, E., Hoffmann, S., Taupin, J. D., Francou, B., Ribstein, P., Caillon, N., Ferron, F. A., Landais, A., Petit, J. R., Pouyaud, B., Schotterer, U., Simoes, J. C., and Stievenard, M.: A new deep ice core from Nevado Illimani (6350 m), Bolivia, *Earth Planet. Sc. Lett.*, 212, 337–350, 2003.
- 25 Risi, C., Bony, S., Vimeux, F., and Jouzel, J.: Water stable isotopes in the LMDZ4 general circulation model: model evaluation for present day and past climates and applications to climatic interpretation of tropical isotopic records, *J. Geophys. Res.*, 115, D12118, doi:10.1029/2009JD013255, 2010.
- 30

Constraining the iLOVECLIM comparison using ($\delta^{18}\text{O}$)

T. Caley et al.

[Title Page](#)[Abstract](#)[Introduction](#)[Conclusions](#)[References](#)[Tables](#)[Figures](#)[⏪](#)[⏩](#)[◀](#)[▶](#)[Back](#)[Close](#)[Full Screen / Esc](#)[Printer-friendly Version](#)[Interactive Discussion](#)

- Roche, D. M.: $\delta^{18}\text{O}$ water isotope in the iLOVECLIM model (version 1.0) – Part 1: Implementation and verification, *Geosci. Model Dev.*, 6, 1481–1491, doi:10.5194/gmd-6-1481-2013, 2013.
- Roche, D. M. and Caley, T.: $\delta^{18}\text{O}$ water isotope in the iLOVECLIM model (version 1.0) – Part 2: Evaluation of model results against observed $\delta^{18}\text{O}$ in water samples, *Geosci. Model Dev.*, 6, 1493–1504, doi:10.5194/gmd-6-1493-2013, 2013.
- Roche, D., Paillard, D., and Cortijo, E.: Constraints on the duration and freshwater release of Heinrich event 4 through isotope modelling, *Nature*, 432, 379–382, 2004a.
- Roche, D., Paillard, D., Ganopolski, A., and Hoffmann, G.: Oceanic oxygen-18 at the present day and LGM: equilibrium simulations with a coupled climate model of intermediate complexity, *Earth Planet. Sc. Lett.*, 218, 317–330, 2004b.
- Roche, D. M., Dokken, T. M., Goosse, H., Renssen, H., and Weber, S. L.: Climate of the Last Glacial Maximum: sensitivity studies and model-data comparison with the LOVECLIM coupled model, *Clim. Past*, 3, 205–224, doi:10.5194/cp-3-205-2007, 2007.
- Rohling, E. J. and Cooke, S.: Stable oxygen and carbon isotope ratios in foraminiferal carbonate, in: *Modern Foraminifera*, edited by: Sen Gupta, B. K., Kluwer Acad., Dordrecht, the Netherlands, 239–258, 1999.
- Rosell-Melé, A. and Prah, F. G.: Seasonality of UK' 37 temperature estimates as inferred from sediment trap data, *Quaternary Sci. Rev.*, 72, 128–136, 2013.
- Rozanski, K., L. Araguas-Araguas, and R. and Gonfiantini.: Isotopic patterns in modern global precipitation, in *Climate Change in Continental Isotopic Records*, edited by: Swart, P. K., *Geophys. Monogr. Ser.*, 78, 1–36, AGU, Washington DC, 1993.
- Rühlemann, C. and Butzin, M.: Alkenone temperature anomalies in the Brazil-Malvinas Confluence area caused by lateral advection of suspended particulate material, *Geochem. Geophys. Geosy.*, 7, Q10015, doi:10.1029/2006GC001251, 2006.
- Sarnthein, M., Gersonde, R., Niebler, S., Pflaumann, U., Spielhagen, R., Thiede, J., Wefer, G., and Weinelt, M.: Overview of Glacial Atlantic Ocean Mapping (GLAMAP 2000), *Palaeoceanography*, 18, 1030, doi:10.1029/2002PA000769, 2003.
- Schmidt, G. A.: Oxygen-18 variations in a global ocean model, *Geophys. Res. Lett.*, 25, 1201–1204, 1998.
- Schmidt, G. A., LeGrande, A. N., and Hoffmann, G.: Water isotope expressions of intrinsic and forced variability in a coupled ocean-atmosphere model, *J. Geophys. Res.*, 112, D10103, doi:10.1029/2006JD007781, 2007.

Constraining the iLOVECLIM comparison using ($\delta^{18}\text{O}$)

T. Caley et al.

[Title Page](#)

[Abstract](#)

[Introduction](#)

[Conclusions](#)

[References](#)

[Tables](#)

[Figures](#)

[⏪](#)

[⏩](#)

[◀](#)

[▶](#)

[Back](#)

[Close](#)

[Full Screen / Esc](#)

[Printer-friendly Version](#)

[Interactive Discussion](#)

- Schmidt, G. A., Annan, J. D., Bartlein, P. J., Cook, B. I., Guilyardi, E., Hargreaves, J. C., Harrison, S. P., Kageyama, M., LeGrande, A. N., Konecky, B., Lovejoy, S., Mann, M. E., Masson-Delmotte, V., Risi, C., Thompson, D., Timmermann, A., Tremblay, L.-B., and Yiou, P.: Using paleo-climate comparisons to constrain future projections in CMIP5, *Clim. Past Discuss.*, 9, 775–835, doi:10.5194/cpd-9-775-2013, 2013.
- Schrag, D. P., Hampt, G., and Murray, D. W.: Pore fluid constraints on the temperature and oxygen isotopic composition of the glacial ocean, *Science*, 272, 1930–1932, 1996.
- Schrag, D. P., Adkins, J. F., McIntyre, K., Alexander, J. L., Hodell, D. A., Charles, C. D., and McManus, J. F.: The oxygen isotopic composition of seawater during the Last Glacial Maximum, *Quaternary Sci. Rev.*, 21, 331–342, 2002.
- Schulz, H., von Rad, U., and Erlenkeuser, H.: Correlation between Arabian Sea and Greenland climate oscillations of the past 110 000 years, *Nature*, 393, 54–57, 1998.
- Sicre, M. A., Labeyrie, L., Ezat, U., Duprat, J., Turon, J. L., Schmidt, S., Michel, E., and Mazaud, A.: Mid-latitude Southern Indian Ocean response to Northern Hemisphere Heinrich events, *Earth Planet. Sc. Lett.*, 240, 724–731, 2005.
- Siddall, M., Hönisch, B., Waelbroeck, C., and Huybers, P.: Changes in deep Pacific temperature during the mid-Pleistocene transition and Quaternary, *Quaternary Sci. Rev.*, 29, 170–181, 2010.
- Sime, L. C., Kohfeld, K. E., Le Quéré, C., Wolff, E. W., de Boer, A. M., Graham, R. M., and Bopp, L.: Southern Hemisphere westerly wind changes during the Last Glacial Maximum: model-data comparison, *Quaternary Sci. Rev.*, 64, 104–120, 2013.
- Shackleton, N. J.: Attainment of isotopic equilibrium between ocean water and benthonic foraminifera genus *Uvigerina*: isotopic changes in the ocean during the last glacial, *Les méthodes quantitatives d'étude des variations du climat au cours du Pleistocène*, Colloque international du CNRS, Gif-sur-Yvette, France, 219, 203–210, 1974.
- Sharp, Z.: *Principles of Stable Isotope Geochemistry*, Pearson Prentice Hall, Upper Saddle River, NJ, 2007.
- Sun, X., Li, X., Luo, Y., and Chen, X.: The vegetation and climate at the last glaciation on the emerged continental shelf of the South China Sea, *Palaeogeogr. Palaeocl.*, 160, 301–316, 2000.
- Thompson, L., Mosley-Thompson, L., Davis, M., Bolzan, J., Yao, T., Gundestrup, N., Wu, X., Klein, L., and Xie, Z.: Holocene-late Pleistocene climatic ice core records from Quinghai-Tibetan Plateau, *Science*, 246, 474–477, 1989.

Constraining the i/LOVECLIM comparison using ($\delta^{18}\text{O}$)

T. Caley et al.

Title Page

Abstract

Introduction

Conclusions

References

Tables

Figures

⏪

⏩

◀

▶

Back

Close

Full Screen / Esc

Printer-friendly Version

Interactive Discussion



Xu, X., Werner, M., Butzin, M., and Lohmann, G.: Water isotope variations in the global ocean model MPI-OM, *Geosci. Model Dev.*, 5, 809–818, doi:10.5194/gmd-5-809-2012, 2012.

Yoshimura, K., Kanamitsu, M., Noone, D., and Oki, T.: Historical isotope simulation using reanalysis atmospheric data, *J. Geophys. Res.*, 113, D19108, doi:10.1029/2008JD010074, 2008.

Zarriess, M. and Mackensen, A.: Testing the impact of seasonal phytodetritus deposition on $\delta^{13}\text{C}$ of epibenthic foraminifer *Cibicidoides wuellerstorfi*: a 31 000 year high-resolution record from the northwest African continental slope, *Palaeoceanography*, 26, PA2202, doi:10.1029/2010PA001944, 2011.

Zhou, J., Poulsen, C. J., Pollard, D., and White, T. S.: Simulation of modern and middle Cretaceous marine $\delta^{18}\text{O}$ with an ocean-atmosphere general circulation model, *Palaeoceanography*, 23, PA3223, doi:10.1029/2008PA001596, 2008.

Table 1. $\delta^{18}\text{O}$ anomaly between the LGM and LH compiled for Greenland, Antarctic ice cores and speleothem records and compared to model (*i*LOVECLIM) results.

Site Name	latitude	longitude	Elevation (m)	References	$\delta^{18}\text{O}$ Op Data LGM-LH (%)	Error Anomaly (2σ)	$\delta^{18}\text{O}$ Op <i>i</i> LOVECLIM LGM-LH (‰)
Camp century	77.18	-61.13	1887	Johnsen et al. (1972)	-12.87		-13.38
GISP	72.58	-38.48	3208	Grootes et al. (1997)	-5.4	1.74	-2.32
GRIP	72.57	-37.62	3232	Johnsen et al. (1997)	-5.73	2.90	-2.32
NGRIP	75.1	-42.32	2917	NGRIP Members (2004)	-7.18	2.06	-8.36
Renland	72	-25	2340	Johnsen et al. (1992)	-5		-2.75
Dye 3	65.18	-43.81	2480	Langway et al. (1985)	-4.5		-1.96
NEMM	77.45	-51 006	2450	NEMM community members (2013)	-7.5		-13.13
BYRD	-80	-120	1530	Blunier and Brook (2001)	-8		-13.59
DomeC	-74.65	124.17	3240	Lorius et al. (1979)	-8.2	1.57	-1.07
EDC	-75	123	3233	Jouzel et al. (2007)	-5.42	0.89	-0.42
EDML	-75	0	2892	EPICA Members (2006)	-7.47		-6.07
Talos Dome	-72.82	159	2315	Stenni et al. (2011)	-4		-5.40
Siple Dome	-81.65	-148.81	621	Brook et al. (2005)	-7		-16.00
WDC	-79.383	-111 239	1791	WAIS Divide Project Members (2013)	-7		-8.64
Vostok	-78	106	3488	Petit et al. (1999)	-4.69	1.49	0.88
Dome F	-77.32	39.7	3810	Kamawura (2007)	-4.46	0.62	-6.54
Dome B	-77.8	94.9		Vaikmae et al. (1993)	-5		-0.19
					$\delta^{18}\text{O}$ Oc Data LGM-LH (%)		$\delta^{18}\text{O}$ Oc <i>i</i> LOVECLIM LGM-LH (‰)
Botuverá Cave	-27.22	-49.16	230	Cruz et al. (2005)	-0.34	0.52	0.55
Cold Air Cave	-24.02	29.11	1375	Holmgren et al. (1999)	1.2	1.61	0.80
Gunung Buda National Park	4.03	114.8	150	Partin et al. (2007)	1.73	0.42	1.66
Jerusalem West Cave	31.78	35.15	700	Frumkin et al. (1999)	1.3	0.48	1.09
NWSI north-west of the South Island	-42	172	700	Williams et al. (2010)	0.29	0.46	1.02
Sofular Cave	41.42	31.93	700	Fleitmann et al. (2009)	-4.57	0.56	0.90
Soreq Cave	31.45	35.03	400	Bar-Matthews et al. (2003)	2.11	0.47	1.09
Kesang Cave	42.87	81.75	2000	Cheng et al. (2012)	1.72	1.81	5.19
Mt. Arthur	-41.28	172.63	390	Hellstrom et al. (1998)	0.93	0.50	1.31
Namibia	-25	18		Stute and Talma (1998)	1.5		1.50

Constraining the *i*LOVECLIM comparison using ($\delta^{18}\text{O}$)

T. Caley et al.

Title Page

Abstract

Introduction

Conclusions

References

Tables

Figures

◀

▶

◀

▶

Back

Close

Full Screen / Esc

Printer-friendly Version

Interactive Discussion

Constraining the *i*LOVECLIM comparison using ($\delta^{18}\text{O}$)

T. Caley et al.

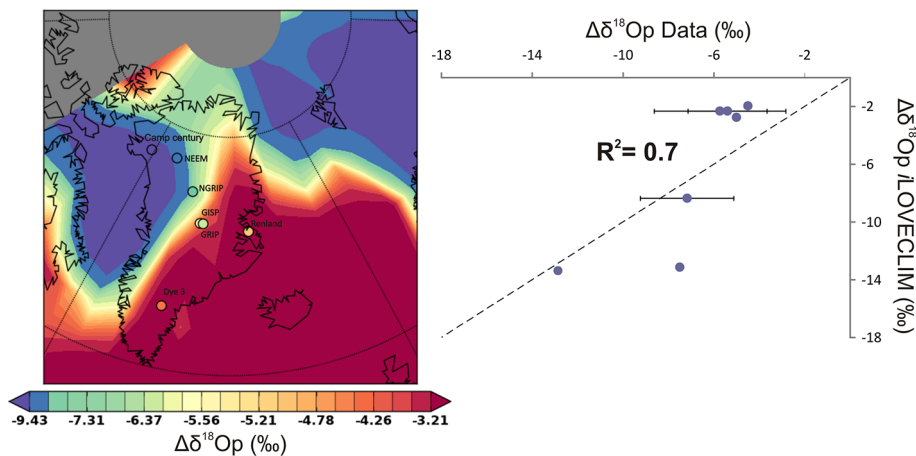


Fig. 2. Comparison between simulated precipitation $\delta^{18}\text{O}$ anomaly (LGM-CT) in *i*LOVECLIM and ice cores data from Greenland (Table 1). Reported uncertainties on data are 2σ .

Title Page

Abstract

Introduction

Conclusions

References

Tables

Figures

⏪

⏩

◀

▶

Back

Close

Full Screen / Esc

Printer-friendly Version

Interactive Discussion

Constraining the *i*LOVECLIM comparison using ($\delta^{18}\text{O}$)

T. Caley et al.

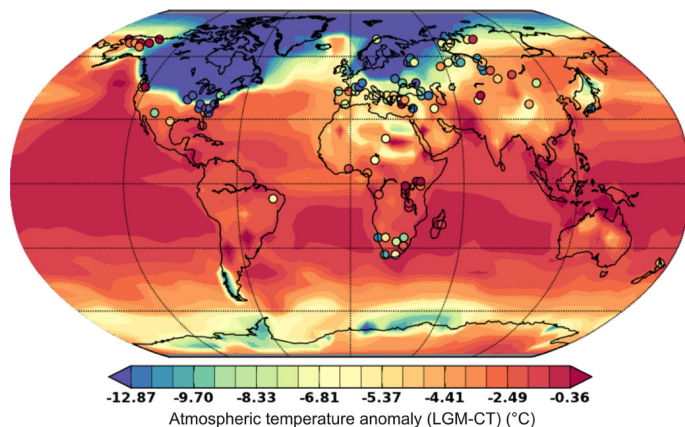


Fig. 4. Comparison between simulated atmospheric temperature anomaly (LGM-CT) in *i*LOVECLIM and pollen-based continental climate reconstructions (Bartlein et al., 2011).

[Title Page](#)[Abstract](#)[Introduction](#)[Conclusions](#)[References](#)[Tables](#)[Figures](#)[⏪](#)[⏩](#)[◀](#)[▶](#)[Back](#)[Close](#)[Full Screen / Esc](#)[Printer-friendly Version](#)[Interactive Discussion](#)

Constraining the *i*LOVECLIM comparison using ($\delta^{18}\text{O}$)

T. Caley et al.

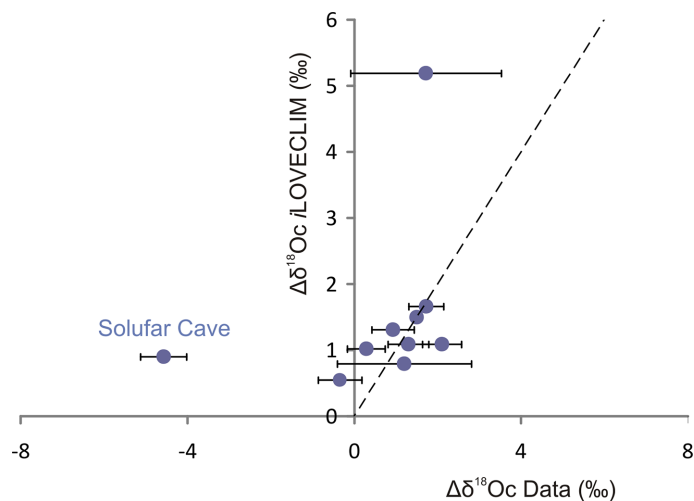


Fig. 5. Comparison between simulated continental calcite $\delta^{18}\text{O}$ anomaly (LGM-CT) in *i*LOVECLIM and global speleothem data (Table 1). Reported uncertainties on data are 2σ .

Title Page

Abstract

Introduction

Conclusions

References

Tables

Figures

⏪

⏩

◀

▶

Back

Close

Full Screen / Esc

Printer-friendly Version

Interactive Discussion



Constraining the *i*LOVECLIM comparison using ($\delta^{18}\text{O}$)

T. Caley et al.

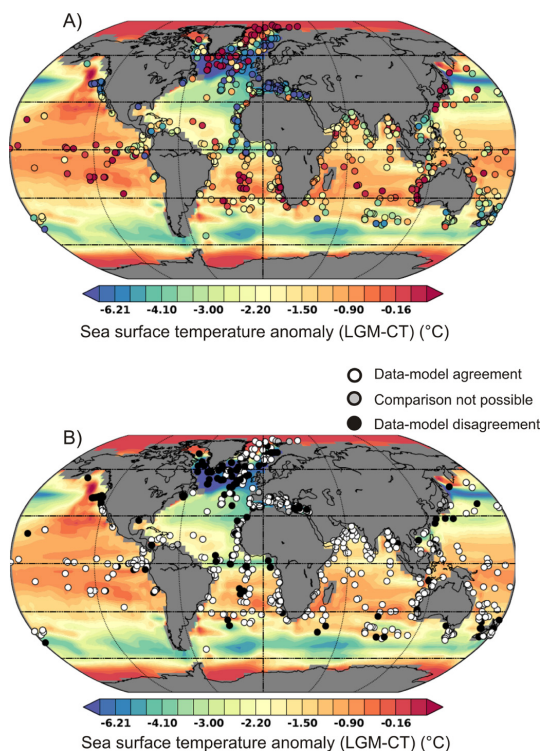


Fig. 6. (A) Comparison between simulated SST anomaly (LGM-CT) in *i*LOVECLIM and MARGO data (MARGO Project Members, 2009). (B) Quantitative agreement or disagreement between simulated SST anomaly (LGM-CT) in *i*LOVECLIM and MARGO data (MARGO Project Members, 2009), taking into account the uncertainties on SST reconstructions. Grey points (comparison not possible) denote the absence of error bars on data or denote locations where model results are not comparable to data (coastal sites).

[Title Page](#)[Abstract](#)[Introduction](#)[Conclusions](#)[References](#)[Tables](#)[Figures](#)[⏪](#)[⏩](#)[◀](#)[▶](#)[Back](#)[Close](#)[Full Screen / Esc](#)[Printer-friendly Version](#)[Interactive Discussion](#)

Constraining the *i*LOVECLIM comparison using ($\delta^{18}\text{O}$)

T. Caley et al.

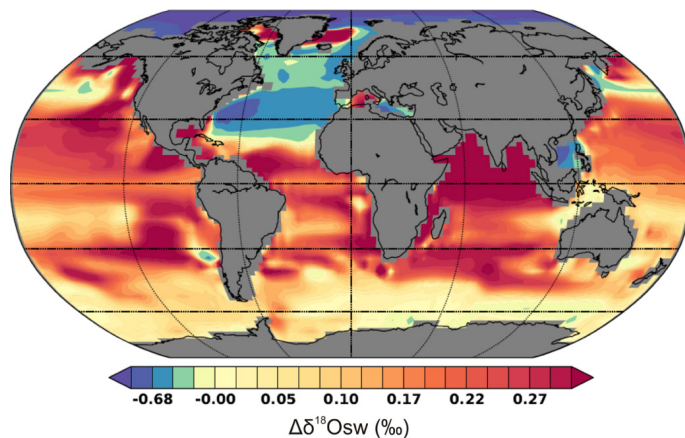


Fig. 7. Simulated surface water $\delta^{18}\text{O}$ anomaly (LGM-CT) in *i*LOVECLIM. A correction of the LGM ice-sheet contribution (1 ‰) has been applied.

[Title Page](#)[Abstract](#)[Introduction](#)[Conclusions](#)[References](#)[Tables](#)[Figures](#)[⏪](#)[⏩](#)[◀](#)[▶](#)[Back](#)[Close](#)[Full Screen / Esc](#)[Printer-friendly Version](#)[Interactive Discussion](#)

Constraining the *i*LOVECLIM comparison using ($\delta^{18}\text{O}$)

T. Caley et al.

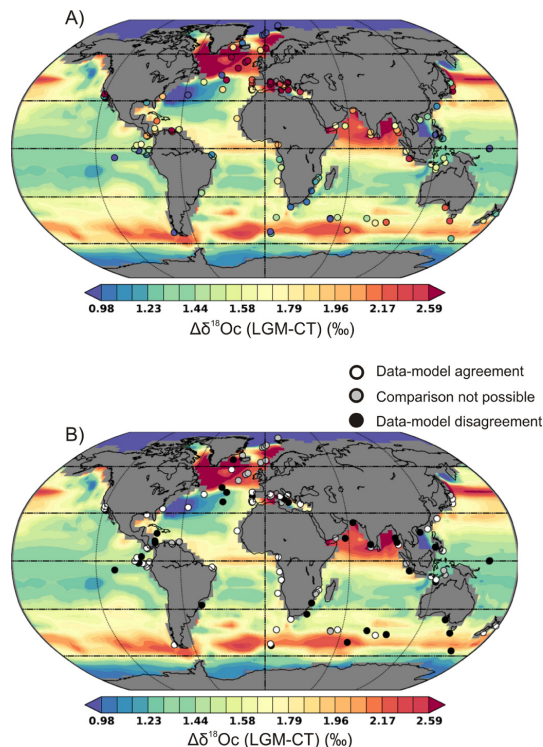


Fig. 8. (A) Comparison between simulated surface ocean calcite $\delta^{18}\text{O}$ calcite anomaly (LGM-CT) in *i*LOVECLIM (0–50 m) and global planktic foraminifera data (Table S1). (B) Quantitative agreement or disagreement between simulated surface ocean calcite $\delta^{18}\text{O}$ anomaly (LGM-CT) in *i*LOVECLIM (0–50 m) and global planktic foraminifera data (Table S1), taking into account the uncertainties on calcite $\delta^{18}\text{O}$ data (2σ). Grey points (comparison not possible) denote the absence of error bars on data or denote locations where model results are not comparable to data (coastal sites).

[Title Page](#)
[Abstract](#)
[Introduction](#)
[Conclusions](#)
[References](#)
[Tables](#)
[Figures](#)
[Back](#)
[Close](#)
[Full Screen / Esc](#)
[Printer-friendly Version](#)
[Interactive Discussion](#)

Constraining the *i*LOVECLIM comparison using ($\delta^{18}\text{O}$)

T. Caley et al.

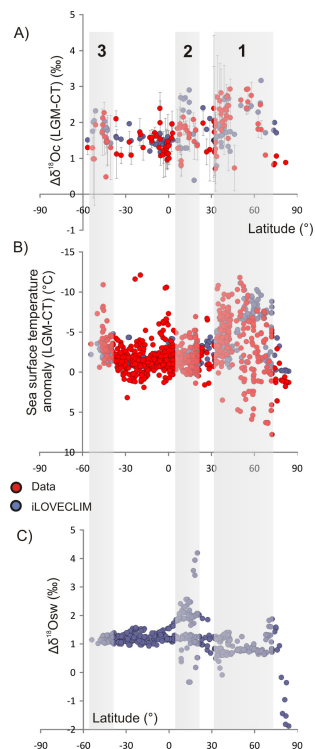


Fig. 9. Data-model (*i*LOVECLIM) comparison as a function of latitude for **(A)** the surface ocean (0–50 m) calcite $\delta^{18}\text{O}$ anomaly (LGM-CT) and **(B)** sea surface temperature anomaly (LGM-CT). **(C)** Simulated surface water $\delta^{18}\text{O}$ anomaly (LGM-CT) in *i*LOVECLIM as a function of latitude (model results are taken at the same location as sea surface temperature data). Grey bands denote large positive calcite $\delta^{18}\text{O}$ anomaly in (1) the north Atlantic, (2) the north Indian Ocean and (3) the Southern ocean as discussed in the text.

Constraining the *i*LOVECLIM comparison using $\delta^{18}\text{O}$

T. Caley et al.

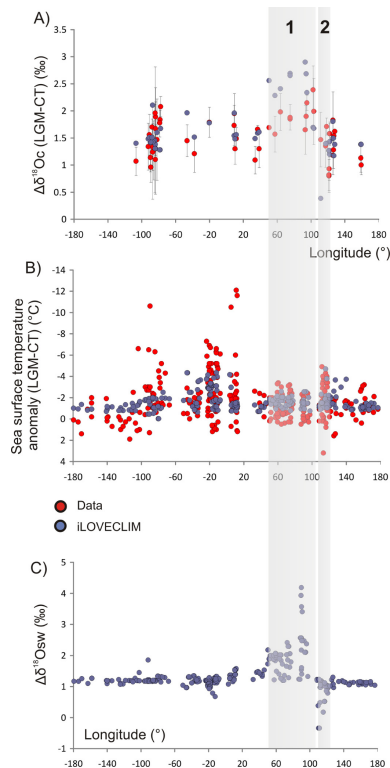


Fig. 10. Data-model (*i*LOVECLIM) comparison as a function of longitude in the tropical band (30° N–30° S) for **(A)** the surface ocean (0–50 m) calcite $\delta^{18}\text{O}$ anomaly (LGM-CT) and **(B)** sea surface temperature anomaly (LGM-CT). **(C)** Simulated surface water $\delta^{18}\text{O}$ anomaly (LGM-CT) in *i*LOVECLIM as a function of longitude in the tropical area (30° N–30° S) (model results are taken at the same location as sea surface temperature data). Grey bands denote large positive/negative calcite $\delta^{18}\text{O}$ anomaly in (1) the north Indian Ocean (2) the China Sea as discussed in the text.

[Title Page](#)[Abstract](#)[Introduction](#)[Conclusions](#)[References](#)[Tables](#)[Figures](#)[⏪](#)[⏩](#)[◀](#)[▶](#)[Back](#)[Close](#)[Full Screen / Esc](#)[Printer-friendly Version](#)[Interactive Discussion](#)

Constraining the *i*LOVECLIM comparison using ($\delta^{18}\text{O}$)

T. Caley et al.

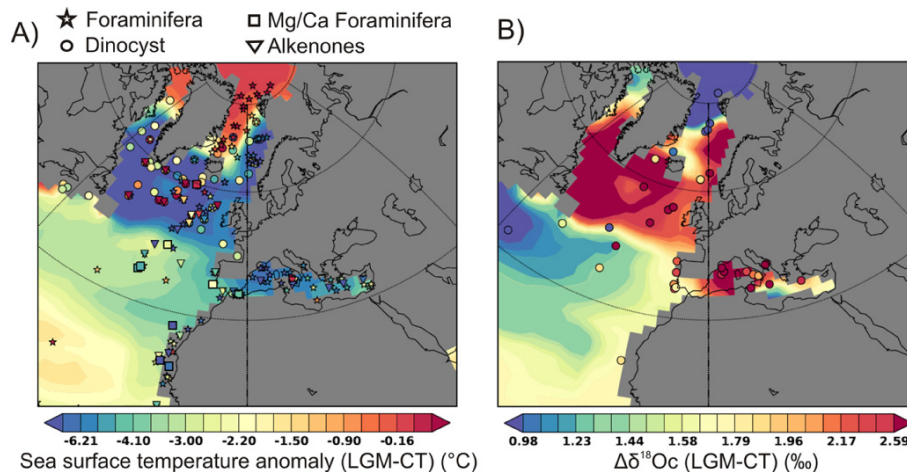


Fig. 11. A focus on the north Atlantic region with **(A)** the comparison between simulated SST anomaly (LGM-CT) in *i*LOVECLIM and MARGO reconstructions for each temperature proxy (MARGO Project Members, 2009). **(B)** The comparison between simulated surface ocean calcite $\delta^{18}\text{O}$ anomaly (LGM-CT) in *i*LOVECLIM (0–50 m) and planktic foraminifera $\delta^{18}\text{O}$ data (Table S1).

Title Page

Abstract

Introduction

Conclusions

References

Tables

Figures

◀

▶

◀

▶

Back

Close

Full Screen / Esc

Printer-friendly Version

Interactive Discussion

Constraining the *i*LOVECLIM comparison using ($\delta^{18}\text{O}$)

T. Caley et al.

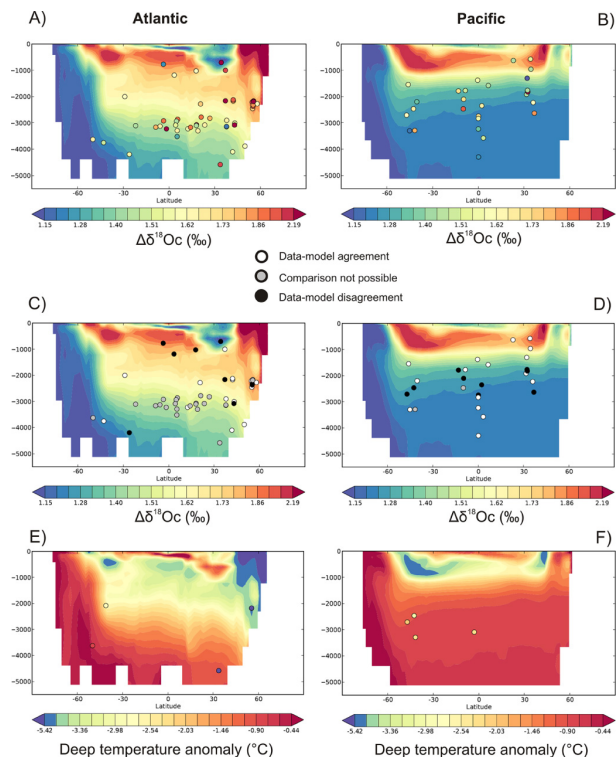


Fig. 13. Atlantic and Pacific zonal mean anomaly (LGM-CT) for **(A)** Atlantic and **(B)** Pacific simulated deep ocean calcite $\delta^{18}\text{O}$ in *i*LOVECLIM and global benthic foraminifera data (Table S2). **(C)** and **(D)** same as **(A)** and **(B)** but taking into account the uncertainties on calcite $\delta^{18}\text{O}$ data (2σ). Grey points (comparison not possible) denote the absence of error bars on data or denote locations where model results are not comparable to data (coastal sites). **(E)** and **(F)** simulated deep temperature in *i*LOVECLIM and deep temperature reconstructions for the Atlantic and for the Pacific Oceans respectively (Adkins et al., 2002; Waelbroeck et al., 2002; Malone et al., 2004; Siddall et al., 2010; Elderfield et al., 2012).